Measurement of Steady-State Minority-Carrier Transport Parameters in Heavily Doped n-Type Silicon

JESÚS A. DEL ALAMO, MEMBER, IEEE, AND RICHARD M. SWANSON, MEMBER, IEEE

Abstract—**The relevant hole transport and recombination parameters in heavily doped n-type silicon under steady state are the hole diffusion length and the product of the hole diffusion coefficient times the hole equilibrium concentration. These parameters have measured in phosphorus-doped silicon grown by epitaxy throughout nearly two orders of magnitude of doping level. Both parameters are found to be strong functions of donor concentration. The equilibrium hole concentration can be deduced from the measurements. A rigid shrinkage of the forbidden gap appears as the dominant heavy doping mechanism in phosphorus-doped silicon.**

I. Introduction

HEAVILY DOPED regions are present in virtually every semiconductor device. Although in many devices they are mere reservoirs of majority carriers to be utilized in an adjacent region, in others the transport and recombination of minority carriers inside the heavily doped region plays a crucial role. That is the case, for example, of bipolar transistors and solar cells. In silicon bipolar transistors the hole current injected into the heavily doped n-type emitter limits the maximum gain achievable from the device [1]. This limitation propagates throughout the design and sets an upper bound to the maximum amplification frequency [2]. Analogously in solar cells, high power conversion efficiency requires as large an open-circuit voltage and internal quantum efficiency to ultraviolet radiation as possible. These figures are to such an extent limited by the recombination prevalent in the heavily doped regions that high efficiencies have only been possible recently by the reduction of the total volume of highly doped semiconductor present in the device [3]. An understanding of minority-carrier physics inside heavily doped semiconductors is imperative for continuing the improvement of the performance of bipolar transistors and solar cells.

Three physical parameters describe the behavior of minority carriers in a heavily doped semiconductor under a wide variety of circumstances [4]. For n-type silicon these parameters are the hole equilibrium concentration p_0, lifetime τ_p, and diffusion coefficient D_p. A number of other parameters have been used in the description of minority carriers in heavily doped semiconductors. Among them, "bandgap narrowing" ΔE_g, "effective intrinsic carrier concentration" n_{ie}, and "effective doping level" $N_{D\text{eff}}$, have become rather popular. These parameters, although sufficient for device modeling, have a doubtful physical significance. In particular, the lack of a physical meaning of the use of bandgap narrowing in transport characterization is stressed by the drastic difference between the results arising from device and optical measurements [5], [6]. We, therefore, prefer in our notation to emphasize the limitations of this parameter when used in transport studies by denoting it "apparent bandgap shrinkage" ΔE_g^{app}.

In steady state, a situation of particular practical importance, only two new parameters, combinations of the fundamental three, are relevant. A particularly useful choice consists of the hole diffusion length $L_p = \sqrt{\tau_p D_p}$, and the product of the hole consists of the hole diffusion coefficient and equilibrium hole concentration $p_0 D_p$ [4]. The measurement of these two parameters in phosphorus-doped silicon is addressed in the present paper.

Many types of device structures have been employed over the years by various authors in the endeavor of measuring the parameters responsible for minority-carrier transport in heavily doped silicon. Although earlier authors extracted, by one way or another, values for bandgap narrowing in heavily doped silicon in bipolar transistors [7], [8], Slotboom and de Graaff [9] were the first to design specific test structures for the measurement of heavy doping parameters in p-type silicon. Their experiment was strictly carried out in the steady state; nevertheless, they choose to report their data as ΔE_g^{app} by making an assumption on the value of D_n, the electron diffusion coefficient.

Wulms [10] extracted values of n_{ie}^2 from I^2L structures. The heavily doped regions were, however, very inhomogeneous in their dopant distribution. An analogous problem is present in the experimental work of Lindholm *et al.* on n^+-p diodes [11], Tang on p-n-p bipolar transistors [12], and Possin *et al.* on n-p-n transistors [13].

Wieder [14] based his determination of n_{ie}^2 and L_p on

Manuscript received July 24, 1986; revised February 2, 1987. This work was supported by the Jet Propulsion Laboratory under Contract 957759.

J. A. del Alamo was with the Solid State Electronics Laboratory, Stanford University, Stanford, CA 94304. He is now with NTT Laboratories, 3-1 Morinosato Wakamiya, Atsugi-shi, Kanagawa, 243-01 Japan.

R. M. Swanson is with the Solid State Electronics Laboratory, Stanford University, Stanford, CA 94305.

IEEE Log Number 8714348.

0018-9383/87/0700-1580$01.00 © 1987 IEEE

lateral p-n-p bipolar transistors fabricated on heavily doped substrates. He made an assumption on the value of D_p since his measuring technique was in the steady state. A similar assumption was made in the electron-beam-induced current (EBIC) work of Possin *et al.* [15] on n-p-n vertical bipolar transistors.

Mertens *et al.* [16] simultaneously measured ΔE_g^{app}, L_p, and D_p from a set of experiments that involved vertical n-p-n bipolar transistors and photodiodes. Neugroschel *et al.* [17] performed temperature-dependent I–V measurements of diodes and transistors with heavily doped emitters. Since the emitters were fabricated by As ion implantation and annealing, the impurity profiles were rather flat. From the temperature dependence of this emitter recombination component they identified the contribution of a ΔE_g^{app} term. Later on they extracted D_p [18].

This intense experimental work has led to a wealth of data. Unfortunately, the as-reported results are highly inconsistent with each other, and large discrepancies exist. A recent analysis has shown that the nature of the disagreements among the results of various authors is due to assumptions made on the interpretation of the data, and not to the data itself [19]. More measurements therefore are necessary to confirm this finding and provide accurate fits to be introduced in device analysis codes.

Among the techniques used in this previous experimental work a clear identification of the ideal measuring structure of $p_0 D_p$ arises. First, the measurement of a collector current in a bipolar transistor is a very clean monitor of the transport of minority carriers through the base. The collector current is ideal with respect to the base–emitter voltage. This fact allows for the easy identification of problems in the measuring process (like temperature estimation) and leads to an accurate extraction of the transport parameters. In addition, no current separation is necessary. When measuring the injected current into a heavily doped emitter, the nonideal recombination component of the depletion region and the ideal recombination contribution of the other side of the junction have to be separated from the total base current. This current separation often needs additional measurements and assumptions, and therefore is more prone to yield large errors in the estimation of the desired component. The measurement of a collector current eliminates this problem.

Second, the heavily doped region has to be as homogeneously doped as possible to have a simplified accurate extraction of the minority-carrier transport parameters. For this reason, epitaxy is the optimum fabrication technique that allows precise doping level and thickness control.

In the process of extraction of ΔE_g^{app} several authors measured the hole diffusion length by various techniques [14]–[16]. Other authors have carried out specific measurements of hole diffusion length. For example, Nijs [20] provides more measurements using the same technique of Mertens *et al.* on heavily doped substrates, while EBIC has also been used [21], [22]. Passari and Susi [23] measured L_p by studying the spectral dependence of the photoelectromagnetic effect and the photoconductive effect (they also made an assumption on D_p and reported their data as τ_p). Of all these techniques for the measurement of L_p, the lateral bipolar transistor structure used by Weider is perfectly compatible with the fabrication of the vertical transistor structures for the measurement of $p_0 D_p$, and therefore they can all be integrated side by side on the same chip. This is the technique selected in this work.

II. Experimental

Fig. 1 shows a cross section of the devices fabricated in this work. In summary, on a p-type substrate, an n^+-epitaxial layer is grown. A p^{++}-region is formed on top by ion implantation and annealing. An n^{++}-region is also formed to provide a contact to the epitaxial layer. On the back of the wafer, a p^{++}-region provides contact to the substrate. All devices are isolated from each other by means of trenches that cut through the epitaxial layer.

In Fig. 1 the top device is a p-n^+-p^{++} bipolar transistor in the vertical direction. This device is used to study the flow of holes through the epitaxial base from the bottom p-substrate, behaving as an emitter, toward the top p^{++}-region, behaving as a collector. From the collector characteristics of this device, the parameter $p_0 D_p$ in the n^+-epitaxial base is extracted, as will be shown later. The bottom device of Fig. 1 is a p^{++}-n^+-p^{++} lateral bipolar transistor along the surface of the epitaxial region. The emitter and collector regions are formed simultaneously to the collector of the vertical transistor. The collector current of each lateral device depends on the separation between the emitter and collector. Since this is easy to control, by simultaneously fabricating several lateral transistors with different spacings, the diffusion length of holes in the epitaxial base can be obtained.

The starting material was ⟨100⟩ orientation 3-in-diameter Si wafers. They were B-doped with a resistivity of 0.2–0.5 Ω · cm. The first step in the device fabrication process was the growth of the epitaxial region with the desired thickness and doping level. The epitaxy was performed at 1050°C in a $SiH_4/PH_3/H_2$ atmosphere [24]. In order to form the top p^{++}-regions, the front side was implanted, through an oxide mask, with a triple dose of B^+ ions: 4×10^{15} cm^{-2} at 100 keV, 3×10^{15} cm^{-2} at 35 keV. BF_2^+ was subsequently implanted on the back of the wafer with a dose of 10^{16} cm^{-2} at 180 keV, to facilitate the contact to the substrate. Both implantations were carried out with the wafer tilted at an angle of 7°.

The n^{++}-base contact regions were formed by phosphorus out-diffusion from a 5000-Å-thick LPCVD P-doped SiO_2 glass. During the same thermal step (1050°C, 30 min, Ar atmosphere), the activation of the ion-implanted species took place. A value of sheet resistance of about 24 Ω/□ was achieved in the front p^{++}-region, while the back p^{++}-region had about 22 Ω/□, and the front n^+-region had around 9 Ω/□.

The isolation trench was performed in a KOH solution. The trench was 100 μm wide and with a depth tailored to the specific wafer. A 800°C 40-min oxidation was per-

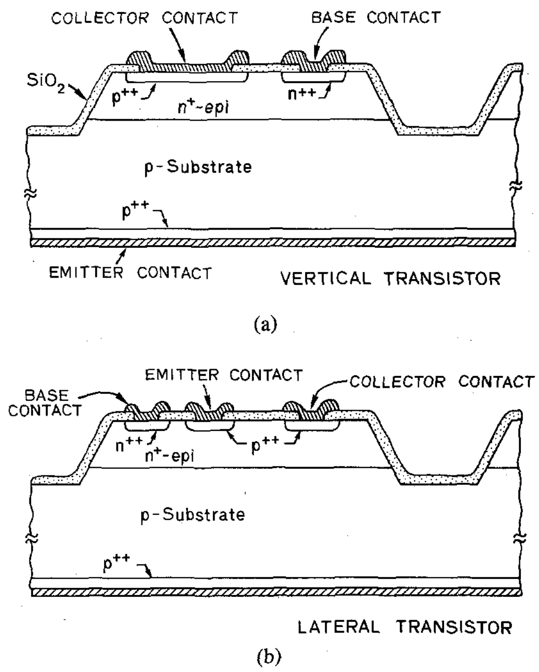

Fig. 1. Schematical cross section of (a) vertical and (b) lateral bipolar transistors.

formed in order to passivate the surface of the lateral transistors for an accurate extraction of L_p [25]. As contact metal, Al was evaporated and annealed at 350°C during 10 min in a forming-gas atmosphere.

Three sizes of vertical transistors were fabricated with $100 \times 100\ \mu m^2$, $200 \times 200\ \mu m^2$, and $500 \times 500\ \mu m^2$ collectors (they are labeled from here on as "small," "medium," and "large"). The set of lateral transistors has a common base and emitter and independent collectors at various distances from the common emitter. Two different sets of devices were simultaneously fabricated. One of them is dedicated to the measurement of small diffusion lengths ($L_p \lesssim 5\ \mu m$). It has nine collectors with the closest at 1.25 μm (drawn distance) from the emitter, and the other ones at distances increasing in 1.25-μm steps, with the ninth one at 11.25 μm. The other set of lateral devices is intended for the measurement of larger diffusion lengths ($L_p > 5\ \mu m$) and has five collectors equally spaced from 10 to 50 μm from the common emitter.

A 4×4 mm^2 van der Pauw structure was also integrated in the same chip to measure the sheet resistance and Hall mobility of the n^+-epitaxial region for an accurate characterization of the phosphorus doping level. A 5×5 mm^2 pad was dedicated to spreading resistance measurements of the vertical impurity profile distributions. The total chip is square with a side of 11 mm. Nine dies are integrated in one wafer. Devices in the central die were usually measured.

The testing of the devices was carried out using an automatic data-acquisition system controlled by an HP 9845 desktop computer. The typical error in the measurement of current and voltage was within 3 percent from 10^{12} to 10^{-2} A and 1 mV to 100 V. The temperature of the sample was estimated by placing a thermocouple under a piece of silicon in the immediate vicinity of the sample under test, and allowing them to reach thermal equilibrium in the dark (typically 5 min). It is accurate to 0.3°C.

III. Results

A. Measurement of Doping Level in the Epitaxial Region

The sheet resistance and Hall mobility were measured in the integrated van der Pauw structure [24], [26] under a magnetic field of 1.12 kG at 23°C. Typical errors in these measurements are smaller than 1 and 4 percent, respectively.

The vertical carrier profile and epitaxial layer thickness was obtained by a spreading resistance with a resolution better than 0.1 μm. A typical result is shown in Fig. 2. The difference between the electrical junction along the vertical dimension and along the beveled surface has been calculated by Hu [27]. For our kind of box profile, he finds a discrepancy of about 6 percent. A computer program was used to correct for the small rounding that occurs at the emitter–base and base–collector junctions, apparent in Fig. 2, as described in [28]. Finally, the value of the Hall scattering factor was used to find the absolute doping level [29]. The typical overall error in the final doping level is around 10 percent, although it increases in the lower doping range due to incertitude in the value of the Hall scattering factor [29].

B. Measurement of Hole Diffusion Length

The lateral transistors operate with the emitter–base junction in forward bias and the collector–base junction short-circuited. To avoid any interaction with the substrate junction, the bottom p-n^+ junction is also short-circuited. Under these conditions, as Fig. 3 schematically indicates, the emitter injects holes into the n^+-base. Some of the injected holes recombine with the large amount of electrons present in the base and some of them are collected by the bottom substrate. A fraction of the injected holes follows a horizontal path close to the surface and are collected by the p^{++} top collector. The magnitude of this collector current depends on the relative size of the hole diffusion length and the lateral base width. By having several collectors at different distances from a common emitter, the hole diffusion length can be measured.

An approximate expression for the collector current of a lateral transistor labeled "i" with base width W_{Bi} is

$$I_{ci} = qAF_L p_0 D_p \frac{1}{L_p} \frac{1}{\sinh\left(\dfrac{W_{Bi}}{L_p}\right)} \left(\exp\frac{qV_{EB}}{kT} - 1\right) \quad (1)$$

where A is the collecting area and F_L is the geometrical factor that accounts for two-dimensional effects. All the other symbols have their usual meaning.

It is convenient to work in the regime in which the base thickness is much longer than a diffusion length $W_{Bi} >>$

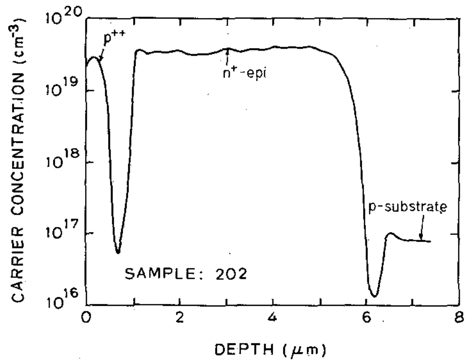

Fig. 2. Vertical carrier concentration profile obtained by spreading resistance.

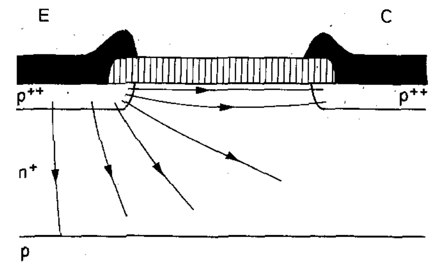

Fig. 3. Illustration of the hole flow from the emitter to the collector in a lateral bipolar transistor.

L_p. In this case the collector saturation current (the pre-exponential term in (1) is

$$I_{oci} = qAF_L p_0 D_p \frac{2}{L_p} \exp -\frac{W_{Bi}}{L_p}. \quad (2)$$

I_{oci} has now an exponential dependence on W_{Bi}. The condition $W_{Bi} >> L_p$ is not so restrictive as appears at first sight. With $W_{Bi} = 2L_p$, the error of (2) with respect to (1) is less than 2 percent.

The ratio of the collector current of two lateral transistors (let us denote them with the subfixes "i" and "1") with a common emitter is

$$\frac{I_{oci}}{I_{oc1}} = \exp -\frac{W_{Bi} - W_{B1}}{L_p}. \quad (3)$$

This ratio is exponentially dependent on the difference of base width with a characteristic constant which is precisely L_p, the hole diffusion length. The advantage of the dependence on the base-width difference is that the as-drawn base widths can be used, rather than the real on-chip width. Although lateral diffusion of B is expected during the thermal step, it occurs in all p^{++}-regions to the same extent. The real base width is narrower than the as-drawn base width; however, the differences of these two base widths in two devices on the same chip is constant.

To reach (3) from (2), the collecting area A and the geometrical factor F_L have to be independent of the geometry of the device and cannot change when W_{Bi} changes. Experimentally and through simple theoretical arguments it was found that the thickness of the epitaxial n^+-region has to be larger than about four diffusion lengths, and the surface recombination velocity of the surface between emitter and collector has to be smaller than about 1×10^4 cm/s. These conditions were checked by a two-dimensional simulation of the lateral transistors performed using PISCES II [25].

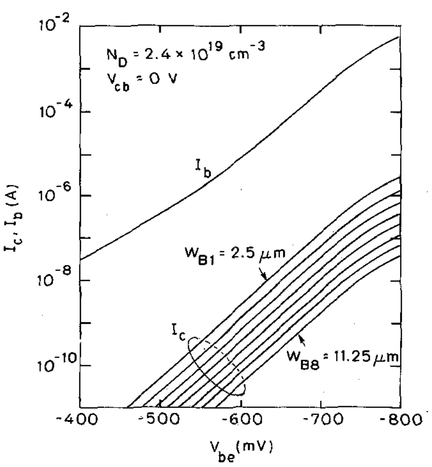

Fig. 4. Gummel plot of a set of lateral devices. There is one common base current and eight collector currents from collectors located at different distances from the emitter.

A typical Gummel plot of one device set is shown in Fig. 4. The figure shows a unique base current for the entire set of devices corresponding to the common base-emitter junction. The collector current of each individual collector is seen to be very ideal with a roll off at high currents due to the influence of series resistance in the base current. The largest collector current corresponds to the narrowest operational device that has an as-drawn base width of $W_{B1} = 2.5$ μm. As the base width increases, the collector current decreases. The spacing between the subsequent collector characteristics is identical in this semilogarithmic plot, which reveals the exponential dependence contained in (2).

The collector saturation current I_{oc} is extracted from the ideal characteristics of Fig. 4 and the knowledge of the temperature. An uncertainty of less than 6 percent exists in the value of I_{oc}. The ratio of the extracted I_{oci}'s is taken with respect to I_{oc1} (corresponding to the device with $W_{B1} = 2.5$ μm). These ratios are then plotted versus $W_{Bi} - W_{B1}$. Some typical results are collected in Fig. 5 in a semilogarithmic plot. From the slope of the straight line portion, the diffusion length is obtained by means of a least squares fitting routine that in all cases gave regression coefficients better than 0.9999.

Fig. 6 collects the results of L_p versus the doping level in the substrate. It is clearly seen that as N_D increases, L_p decreases very strongly. Table 1 contains the numerical values plotted in Fig. 6.

C. Measurement of $p_0 D_p$

The vertical transistors operate with the base–emitter junction in forward bias and the base–collector junction short-circuited. As Fig. 7 indicates, holes are injected from the substrate into the epitaxial base region and some

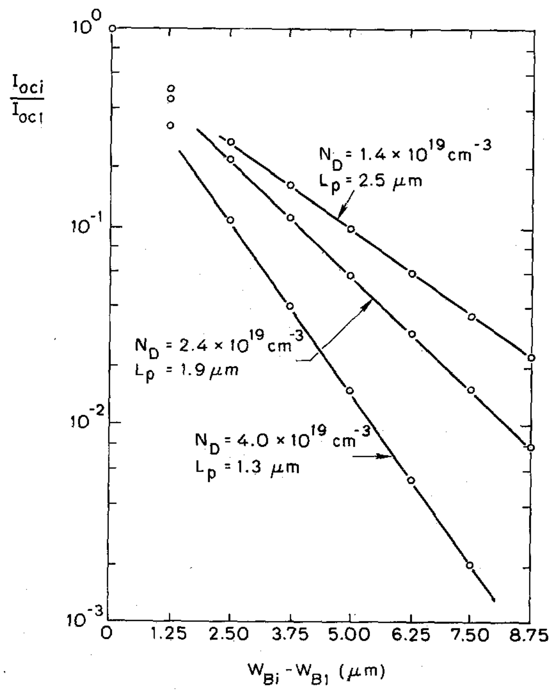

Fig. 5. Ratio of collector saturation currents of device i and device 1 (W_{B1} = 2.5 μm) versus the difference in "as-drawn" base widths, for different devices.

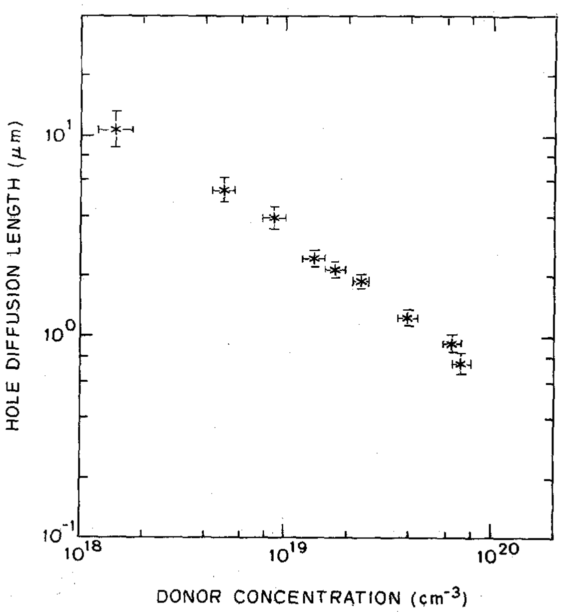

Fig. 6. Measured hole diffusion length versus doping level (T = 292 K).

of them are collected by the top p^{++}-region. The device works in the upward mode so that the collector area is well defined and is smaller than the emitter area. In this way, the flow of holes is expected to be highly one-dimensional all around the collector. Two-dimensional collection may occur along the periphery of the collector, as indicated in an exaggerated way in Fig. 7. To separate this perimeter-collected current from the area-collected current, three devices with three different collector sizes were integrated together.

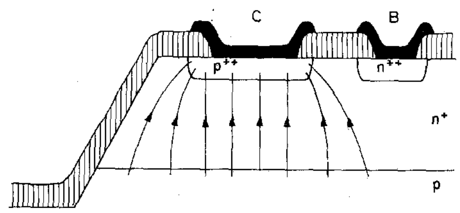

Fig. 7. Illustration of the hole flow from the emitter (substrate) to the collector in a vertical bipolar transistor.

TABLE I
DIFFUSION LENGTH MEASUREMENTS PLOTTED IN FIG. 6

N_D (cm^{-3})	L_p (μm)
1.5×10^{18}	11
4.9×10^{18}	5.2
8.6×10^{18}	3.9
1.4×10^{19}	2.5
1.8×10^{19}	2.1
2.4×10^{19}	1.9
4.0×10^{19}	1.3
6.5×10^{19}	0.92
7.2×10^{19}	0.63

The area-related component of the collector current is

$$I_c = qA_c p_0 D_p \frac{1}{L_p} \frac{1}{\sinh \frac{W_B}{L_p}} \left(\exp \frac{qV_{EB}}{kT} - 1 \right). \quad (4)$$

The collector saturation current density is

$$J_{oc} = qp_0 D_p \frac{1}{L_p} \frac{1}{\sinh \frac{W_B}{L_p}} \quad (5)$$

where W_B now indicates the vertical base width.

In the case that the base width is much smaller than a diffusion length, $W_B << L_p$, then

$$J_{oc} = qp_0 D_p \frac{1}{W_B}. \quad (6)$$

The condition $W_B << L_p$ is not very restrictive, i.e., if $W_B = 0.5\ L_p$ the error in (6) over the exact (5) is about 4 percent, and if $W_B = L_p$, the error is still only 15 percent.

The mode of operation contained in (6) is ideal for the measurement of the parameter $p_0 D_p$. Equation (6) depends linearly on W_B and is independent of L_p. The errors in the extraction of $p_0 D_p$ in this mode of operation are expected to be small. However, as found in the previous section, the diffusion length becomes very short at high doping levels. The condition $W_B < L_p$ becomes rather difficult to fulfill if L_p is of the order of 2 μm or less because of the difficulty of fabricating a heavily doped base with a flat profile of such a small width.

If, however, $W_B >> L_p$, (5) becomes

$$J_{oc} \simeq p_0 D_p \frac{2}{L_p} \exp -\frac{W_B}{L_p}. \quad (7)$$

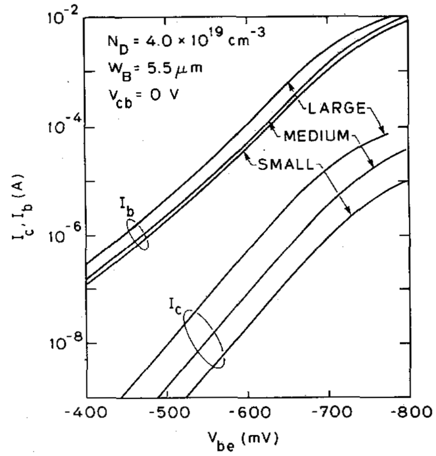

Fig. 8. Gummel plot of three vertical bipolar transistors integrated together on the same chip. For each device, the base and collector currents are indicated.

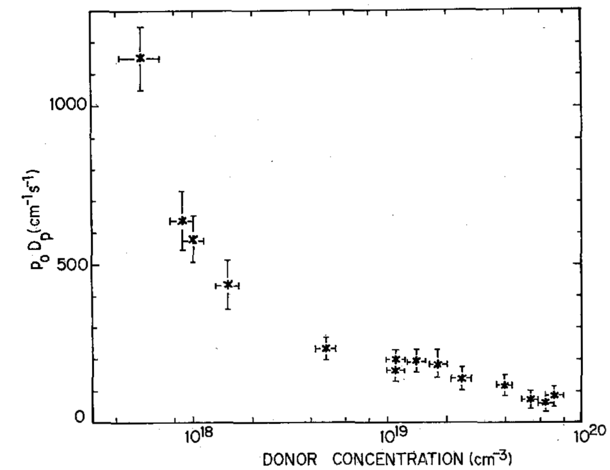

Fig. 9. Measured equilibrium hole concentration times diffusion coefficient product versus doping level ($T = 292$ K).

In this other extreme of operation, J_{oc} is exponentially dependent on both W_B and L_p. There is not only a need to know L_p, but the extraction of the value of $p_0 D_p$ depends exponentially on it. For example, for typical conditions (if $W_B = 5$ μm and $L_p = 1$ μm), an error of 6 percent in L_p becomes an error of about 25 pecent in $p_0 D_p$. The same situation occurs also with W_B. Errors of this order are expected in the values of $p_0 D_p$ for doping levels higher than about $N_D = 2 \times 10^{19}$ cm^{-3} where the mode of operation described by (7) is used. In this case, L_p is determined from the lateral transistor structures that are located at an average distance of 2 mm from the vertical devices.

Fig. 8 shows a typical Gummel plot of a set of the three different vertical devices. The collector current is ideal except for series resistance. The base current, on the other hand, shows strong nonidealities at low voltages that leave a very small ideal region before series resistance effects become important. This figure highlights the importance of designing devices that use the collector current as a measuring tool rather than the base current frequently used by other authors.

From these collector characteristics, the collector saturation current is obtained by least squares fitting for the three devices. The perimeter- and area-related components of the collector current are subsequently separated. The perimeter-collected component was found to contribute a very small part. For example, for the large device (500×500 μm^2 collector), the perimeter component always contributed less than 5 percent of the total collected current. Due to this dominance of the area-related component, the error introduced in the current separation is estimated to be negligible.

Having obtained J_{oc}, the extraction of $p_0 D_p$ can be carried out using (5)–(7). Small corrections over these equations are still necessary to account for the rounding of the base impurity profile produced by P diffusion into the substrate during the high-temperature steps of fabrication. The procedure is described in [25].

All the measurements reported here were carried out at temperatures between 18.9 and 20.3°C. Since the temperature difference from sample to sample is so small, all the data are reported in the same graph without labeling each sample. Fig. 9 collects the resulting $p_0 D_p$ transport parameters versus doping level in the base. Table II contains the numerical values shown in Fig. 9. Although $p_0 D_p$ decreases very fast at low doping levels, the onset of heavy doping effects results in a flattening of $p_0 D_p$ in the high doping regime. These relatively large values of $p_0 D_p$ at high doping levels are responsible for the increased current in heavily doped emitters of bipolar transistors and solar cells.

TABLE II

NUMERICAL VALUES OF DATA PLOTTED IN FIGS. 9, 11–13

N_D (cm^{-3})	T_m (°C)	$p_o D_p$ (s^{-1}cm^{-1})	$n_{io}^2/p_o D_p$ (s·cm^{-5})	p_o (cm^{-3})	ΔE_g^{app} (meV)
5.4×10^{17}	20.3	1150	5.9×10^{16}	127	0.3
8.8×10^{17}	19.6	637	9.3×10^{16}	83	5.3
9.9×10^{17}	19.6	577	1.0×10^{17}	79	7.1
1.5×10^{18}	19.7	437	1.4×10^{17}	71	14
4.8×10^{18}	19.6	233	2.5×10^{17}	56	38
1.1×10^{19}	19.6	203	2.9×10^{17}	56	59
1.1×10^{19}	19.6	166	3.6×10^{17}	46	54
1.4×10^{19}	19.6	196	3.0×10^{17}	56	65
1.8×10^{19}	19.6	186	3.2×10^{17}	54	71
2.4×10^{19}	19.9	139	4.5×10^{17}	41	70
4.0×10^{19}	19.8	116	5.3×10^{17}	35	79
5.4×10^{19}	18.9	76	6.9×10^{17}	23	80
6.5×10^{19}	19.7	63	9.5×10^{17}	19	76
7.2×10^{19}	19.6	83	7.1×10^{17}	25	86

IV. DISCUSSION

A. Numerical Fits to L_p and $p_0 D_p$

The transport parameters L_p and $p_0 D_p$ are sufficient for the accurate modeling of the steady-state current injected into the emitter of bipolar transistors and solar cells. This has been illustrated in [30] where modeling of several accurately characterized heavily doped emitters was demonstrated, without any adjustable parameters, within 30 percent. To this aim, numerical fits to the data obtained in this work and that of other authors have been calculated.

Fig. 10 collects the measurements of L_p in heavily doped n-type Si known to these authors [14]–[16], [20]–[23] and our own, obtained as described above. All the hole diffusion length measurements show good agreement, giving a very tight doping level distribution. Discrepancies of a factor smaller than two are observed, except at the higher doping level limit. The EBIC measurement of Burk and de la Torre [22] probably becomes inaccurate when the generation radius of the electronic beam is comparable to a diffusion length.

The solid line in Fig. 10 is a fit to all values of L_p reported here. The equation is

$$L_p = 2.27 \times 10^{14}\, N_D^{-0.941}\ \text{cm}. \tag{8}$$

Since L_p is especially process dependent at low doping levels, no effort has been made to obtain a fit at this range.

With regard to $p_0 D_p$, the situation is not so simple. Although most previous authors carried out only steady-state measurements, and therefore obtained $p_0 D_p$, they reported their data as (apparent) bandgap narrowing ΔE_g^{app}. To be able to make such step, assumptions were necessary. It is precisely the different nature of the various assumptions taken by different authors that lead to the chaotic picture of ΔE_g^{app} that was described in [19]. In a number of cases, we were able to reconstruct the original $p_0 D_p$ measurements from information provided by the original authors. The procedure was described in detail in [19] and will not be repeated here.

The comparison of all these data (reported at 300 K) with our own is still straightforward because of the different measurement temperatures. p_0, in fact, is a very strong function of temperature, with an activation energy of the order of the Si bandgap, around 1.1 eV. The ratio $p_0 D_p / n_{i0}^2$, however, removes most of that temperature dependence because n_{i0}^2 also has an activation energy of the order of the bandgap. Since the temperature difference between all data is at most 8°C, this ratio is a good basis of comparison.

Fig. 11 shows $n_{i0}^2 / p_0 D_p$ and indicates the degree of agreement that all original measurements of $p_0 D_p$ had reached, i.e., within 30 percent. In fact, this difference of 30 percent in $n_{i0}^2 / p_0 D_p$ translates to a difference in ΔE_g^{app} of about 10 meV. This is a significant improvement over the 70-meV discrepancies of the as-reported data collected in [19]. The solid line in Fig. 11 is a fit to $n_{i0}^2 / p_0 D_p$ versus doping level that is valid for small excursions around 300 K, where the fit is done. The empirical equation is

$$\frac{n_{i0}^2}{p_0 D_p} = 1.620 \times 10^{-3}\, N_D^{1.109}\ \text{s} \cdot \text{cm}^{-5}, \qquad N_D \le 7 \times 10^{17}\ \text{cm}^{-3}$$
$$= 1.431 \times 10^{17} \ln N_D - 5.780 \times 10^{18}\ \text{s} \cdot \text{cm}^{-5}, \quad N_D \ge 7 \times 10^{17}\ \text{cm}^{-3}. \tag{9}$$

This fit has been adjusted to give the proper values of $n_{i0}^2 / p_0 D_p$ at low dopings where heavy doping effects are not important. The exponent of N_D slightly larger than unity in the low doping range accounts for the small decrease of the diffusion coefficient that occurs as the doping level increases.

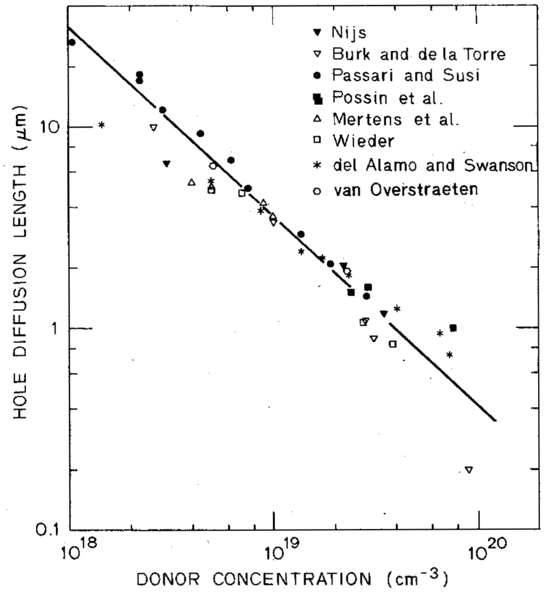

Fig. 10. Experimental data of hole diffusion length versus donor concentration. The line is the empirical fit given by (8).

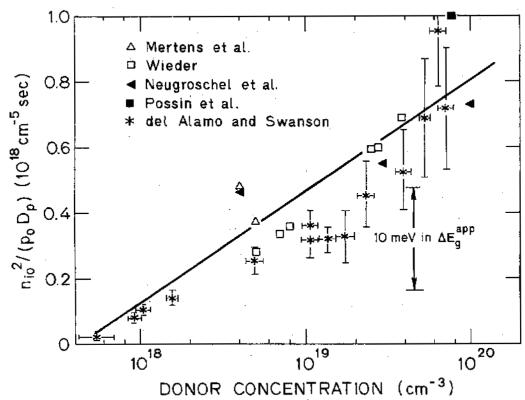

Fig. 11. Experimental data of $n_{i0}^2 / p_0 D_p$ from various authors. The measurement temperature is 300 K for all authors except for the present ones which is 292 K. The solid line is the fit described by (9) at 300 K.

B. Extraction of the Equilibrium Hole Concentration

To deduce the value of p_0 from the $p_0 D_p$ measurements, knowledge of D_p is required. Recently Swirhun and other authors [31], [32] have reported simultaneous measurements of the hole diffusion length and hole lifetime in some of the samples described in this work. The combination of both techniques lead to the measurement of the hole diffusion coefficient in the 10^{19}-cm^{-3} doping regime.

Our D_p measurements and those of other authors allowed the calculation of a curve fit that gave a description of the behavior of D_p within the measurement error, from low doping levels to close to 10^{20}-cm^{-3} donor concentrations [31], [32].

Using this recent knowledge of the hole diffusion coefficient, from the data collected in Fig. 9 we have extracted the value of p_0 and plotted it in Fig. 12. In this figure, the effects of heavy doping are dramatically seen. p_0 in heavily doped silicon has a much higher value than expected from the low-doping theory, shown by a continuous line (the theory uses the correct Fermi–Dirac statistics). The increase in the measured p_0 is at certain doping levels as high as a factor of 30 over the theoretical expectation. This fact implies that for a given disequilibrium at a p-n junction, the hole current injected into an n^+-region will also be higher by the same amount.

The physical origin of this higher equilibrium concentration of holes present in heavily doped n-type silicon is a source of intense research and discussion. Several phenomena seem to be involved that could result in such an increase of p_0, but their correct magnitude is not adequately established. A rigid shrinkage of the Si bandgap and a change in the density of states of the conduction and valence bands are hypothesis that are being contemplated.

While there is never an experimental technique that can completely isolate any of these diverse physical phenomena, photoluminescence [33]–[35] has been shown to constitute a powerful experimental technique for the study of the band structure of heavily doped silicon. It permits the estimation of the penetration of the Fermi level inside the conduction band (in n-type silicon) and the magnitude of the rigid shrinkage of the bandgap. Based on recent reported measurements at low temperatures [33]–[35], we have estimated [25] the equilibrium hole concentration that the rigid bandgap shrinkage measured by photoluminescence would imply. A number of assumptions are involved in a calculation of this nature that forces us to regard its result as an order-of-magnitude indication of the relevant physics. Nevertheless, given the state of knowledge of the band structure of heavily doped silicon, the result of this theoretical calculation gives interesting conclusions.

Indeed, in Fig. 12 the result of the value of p_0 implied by the band structure deduced from photoluminescence measurements is drawn as a broken line. Order of magnitude agreement of this result with our experimental measurements is obtained. This fact points toward rigid bandgap shrinkage being the most important phenomena affecting the band structure of heavily doped silicon. Moreover, the small but consistent 30–50-percent smaller predicted p_0, in comparison to the measured value, may indicate the presence of a small tail at the top of the valence band that increases the density of holes at lower hole energies (higher electron energies). A more detailed calculation of this effect requires assumptions that are difficult to verify experimentally and are out of the scope of this work.

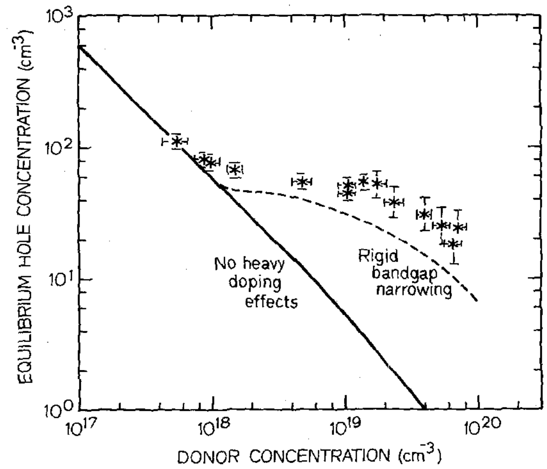

Fig. 12. Equilibrium hole concentration versus donor concentration obtained in this work at 292 K. The solid line represents the theoretical calculation of p_0 without heavy doping effects. The dashed line includes rigid bandgap narrowing determined by photoluminescence.

C. Deduction of ΔE_g^{app} for Device Modeling

The fact that the temperature dependence of p_0 is not known and the fact that most device modeling codes use as a parameter the position-dependent bandgap of the material, rather than the concentration of minority carriers in equilibrium, makes it convenient to deduce a value of "apparent bandgap narrowing" that describes the increment of p_0. We use the following definition for it:

$$\Delta E_g^{app} = kT \ln \frac{p_0 N_D}{n_{i0}^2}. \tag{10}$$

In this equation, complete activation of the dopant atoms is assumed. This is certainly the case above the metal-insulator transition in P-doped silicon, about 3.7×10^{18} cm^{-3}. Below this doping level, partial deionization may occur but to a very small scale at room temperature [29].

We cannot overemphasize enough the fact that (10) is a mere definition without any physical significance. In fact, other authors [17] use a different definitions for ΔE_g^{app} that highlights the need to use Fermi–Dirac statistics for describing the majority carriers. Care has to be taken when using experimental reports of ΔE_g^{app} to use the data defined in the same way as the code in which it is going to be introduced. Using (10), the p_0 data of Fig. 12 can be converted in ΔE_g^{app}. Fig. 13 collects the resulting ΔE_g^{app} versus doping level. The same procedure has been applied to the data of the other authors collected in Fig. 11 at their respective temperatures, and using for all of them the same D_p value given in [32]. A fit to the values of ΔE_g^{app} of Fig. 3 is

$$\Delta E_g^{app} = 18.7 \times 10^{-3} \ln \frac{N_D}{7 \times 10^{17}} \text{ eV}, \quad N_D > 7 \times 10^{17} \text{ cm}^{-3}$$
$$= 0, \quad N_D \leq 7 \times 10^{17} \text{ cm}^{-3}. \tag{11}$$

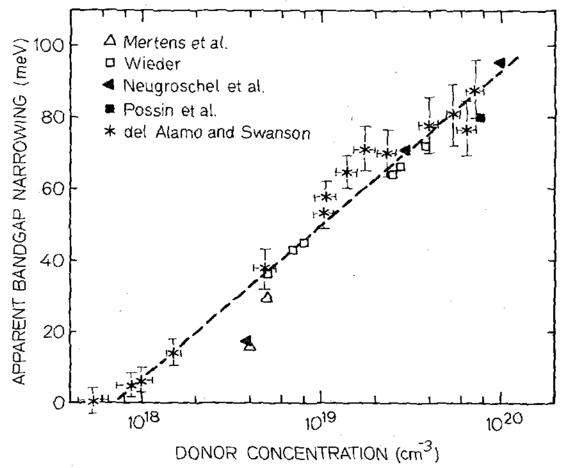

Fig. 13. Apparent bandgap narrowing as defined by (10). The dashed line is described by (11).

This fit, combined with the fit to D_p given in [31], [32] gives the correct product $n_{i0}^2/p_0 D_p$ fitted in (9) within 17 percent, which is smaller than the typical uncertainty in most experimental data.

V. Conclusions

The steady-state transport and recombination parameters of holes in heavily doped epitaxial n-type silicon, diffusion length and equilibrium hole concentration times diffusion coefficient product, have been measured versus the doping level. The doping range covers nearly two orders of magnitude up to almost 7×10^{19} donors/cm^3. Agreement with previous authors is found within a factor of two. The equilibrium hole concentration deduced from our measurements, when compared with calculations based on recently measured rigid bandgap shrinkage by photoluminescence, establishes the rigid narrowing of the bandgap as the dominant heavy doping effect in n-type silicon.

Acknowledgment

The fabrication and testing of the devices described was carried out at the Integrated Circuits Laboratory, where considerable help was received from Dr. J. Shott, M. Prisbe, R. King, T. Van Hooydonk, L. Meisenbach, and D. Roman.

References

[1] T. H. Ning and R. D. Issac, "Effect of emitter contact on current gain of silicon bipolar devices," *IEEE Trans. Electron Devices*, vol. ED-27, pp. 2051–2055, Nov. 1980.

[2] T. Sakai, S. Konaka, Y. Yamamoto, and M. Suzuki, "Prospects of SST technology for high speed LSI," in *IEDM Tech. Dig.*, pp. 18–21, 1985.

[3] R. A. Sinton, Y. Kwark, S. E. Swirhun, and R. M. Swanson, "Silicon point contact concentrator solar cells," *IEEE Electron Device Lett.*, vol. EDL-6, pp. 405–407, Aug. 1985.

[4] J. del Alamo and R. M. Swanson, "Modelling of minority carrier transport in heavily doped silicon emitters," presented at the U.S.-Belgium Joint Seminar on New Developments in the Physics of Homo- and Heterojunctions, Leuven, Belgium, May 1986; to be published in *Solid-State Electron.*, 1987.

[5] R. W. Keyes, "The energy gap of impure silicon," *Commun. Solid State Phys.*, vol. 7, no. 6, pp. 149–156, 1977.

[6] J. del Alamo, R. M. Swanson, and A. Lietoila, "Photovoltaic measurement of bandgap narrowing in moderately doped silicon," *Solid-State Electron.*, vol. 26, no. 5, pp. 483–489, 1983.

[7] R. B. Fair, "Optimum low-level injection efficiency of silicon transistors with shallow arsenic emitters," *IEEE Trans. Electron Devices*, vol. ED-20, pp. 642–647, July 1973.

[8] P. J. Kannam, "Effect of emitter doping on device characteristics," *IEEE Trans. Electron Devices*, vol. ED-20, pp. 845–851, Oct. 1973.

[9] J. W. Slotboom and H. C. de Graaff, "Measurements of bandgap narrowing in Si bipolar transistors," *Solid-State Electron.*, vol. 19, pp. 857–862, 1976.

[10] H. E. J. Wulms, "Base current of I^{2}L transistors," *IEEE J. Solid-State Circuits*, vol. SC-12, pp. 143–150, Feb. 1977.

[11] F. A. Lindholm, A. Neugroschel, C.-T. Sah, M. P. Godlewski, and H. W. Brandhorst, Jr., "A methodology for experimentally based determination of gap shrinkage and effective lifetimes in the emitter and base of p-n junction solar cells and other p-n junction devices," *IEEE Trans. Electron Devices*, vol. ED-24, pp. 402–410, Apr. 1977.

[12] D. D. Tang, "Heavy doping effects in p-n-p bipolar transistors," *IEEE Trans. Electron Devices*, vol. ED-27, pp. 563–570, Mar. 1980.

[13] G. E. Possin, M. S. Adler, and B. J. Baliga, "Measurement of heavy doping parameters in silicon by electron-beam-induced current," *IEEE Trans. Electron Devices*, vol. ED-27, pp. 983–990, May 1980.

[14] A. W. Wieder, "Emitter effects in shallow bipolar devices: Measurements and consequences," *IEEE Trans. Electron Devices*, vol. ED-27, pp. 1402–1408, Aug. 1980.

[15] G. E. Possin, M. S. Adler, and B. J. Baliga, "Measurements of p-n product in heavily doped epitaxial emitters," *IEEE Trans. Electron Devices*, vol. ED-31, pp. 3–17, Jan. 1984.

[16] R. P. Mertens, J. L. Meerbergen, J. F. Nijs, and R. J. Van Overstraeten, "Measurement of the minority-carrier transport parameters in heavily doped silicon," *IEEE Trans. Electron Devices*, vol. ED-27, pp. 949–955, May 1980.

[17] A. Neugroschel, S. C. Pao, and F. A. Lindholm, "A method for determining energy gap narrowing in highly doped semiconductors," *IEEE Trans. Electron Devices*, vol. ED-29, pp. 894–902, May 1982.

[18] A. Neugroschel and F. A. Lindholm, "Evidence for low diffusivity and mobility of minority carriers in highly doped Si and interpretation," *Appl. Phys. Lett.*, vol. 42, no. 2, pp. 176–178, 1983.

[19] J. del Alamo, S. Swirhun, and R. M. Swanson, "Measuring and modelling minority carrier transport in heavily doped silicon," *Solid-State Electron.*, vol. 28, no. 1, pp. 47–54, 1985.

[20] J. Nijs, "Theoretical and experimental study of physical parameters and efficiency limits factors in single crystalline silicon junction solar cells," Ph.D. dissertation, Katholieke Universiteit Leuven, Belgium, 1982.

[21] R. J. Van Overstraeten, private communication, 1984.

[22] D. E. Burk and V. de la Torre, "An empirical fit to minority hole mobilities," *IEEE Electron Device Lett.*, vol. EDL-5, pp. 231–233, July 1984.

[23] L. Passari and E. Susi, "Recombination mechanisms and doping density in silicon," *J. Appl. Phys.*, vol. 54, no. 7, pp. 3935–3937, 1983.

[24] J. del Alamo and R. M. Swanson, "Fabrication and characterization of epitaxial heavily phosphorus-doped silicon," *J. Electrochem. Soc.*, vol. 132, no. 12, pp. 3011–3016, 1985.

[25] J. del Alamo, "Minority carrier transport in heavily doped n-type silicon," Ph.D. dissertation, Stanford Univ., 1985.

[26] L. J. van der Pauw, "A method of measuring the resistivity and Hall coefficient on lamellae of arbitrary shape," *Phillips Tech. Rev.*, vol. 20, no. 8, pp. 220–224, 1958–1959.

[27] S. M. Hu, "Between carrier distributions and dopant atomic distribution in beveled silicon substrates," *J. Appl. Phys.*, vol. 53, no. 3, pp. 1499–1510, 1982.

[28] J. del Alamo and R. M. Swanson, "Measurement of electron mobility in epitaxial heavily-phosphorus-doped silicon," *J. Appl. Phys.*, vol. 56, no. 6, pp. 2250–2252, 1984; correction in *J. Appl. Phys.*, vol. 57, no. 6, p. 2346, 1985.

[29] ——, "Measurement of Hall scattering factor in phosphorus-doped silicon," *J. Appl. Phys.*, vol. 57, no. 6, pp. 2314–2317, 1985.

[30] ——, "Measurement of heavy doping parameters in n-type silicon," in *Proc. 18th IEEE Photovoltaic Specialists Conf.* (Las Vegas, NV), pp. 584–589, 1985.

[31] J. del Alamo, S. Swirhun, and R. M. Swanson, "Simultaneous measurement of hole lifetime, hole mobility, and bandgap narrowing in heavily doped n-type silicon," in *IEDM Tech. Dig.*, pp. 290–293, 1985.

[32] S. E. Swirhun, J. del Alamo, and R. M. Swanson, "Measurement of

hole mobility in heavily doped n-type silicon," *IEEE Electron Device Lett.*, vol. EDL-7, pp. 168-171, Mar. 1986.
[33] P. E. Schmid, M. L. W. Thewalt, and W. P. Dumke, "Photoluminescence in heavily doped Si:B and Si:As," *Solid-State Commun.*, vol. 38, no. 11, pp. 1091-1093, 1981.
[34] J. Wagner, "Photoluminescence and excitation spectroscopy in heavily doped n- and p-type silicon," *Phys. Rev. B*, vol. 29, no. 4, pp. 2002-2009, 1984.
[35] ——, "Heavily doped silicon studied by luminescence and selective absorption," *Solid-State Electron.*, vol. 28, no. 1, pp. 25-30, 1985.

*

Jesüs A. del Alamo (S'79-M'85) was born in Soria, Spain, in 1957. He received the Ingeniero Superior de Telecommunicación degree from the Universidad Politécnica de Madrid, Spain, in 1980 and the M.S. degree in electrical engineering from Stanford University, CA, in 1983. He is currently working toward the Ph.D. degree in electrical engineering at Stanford University. His Ph.D. dissertation concerns the optical and transport properties of heavily doped silicon.

From 1977 to 1981, he was a Research Assistant at the Instituto de Energía Solar of the Unversidad Politécnica de Madrid. His activities there included research on the physics, modeling, and technology bifacial monocrystalline silicon solar cells. A new solar cell was conceived by his research group that is today in production in Spain. During successive summers he has been a Visiting Student at the following institutions: the University of Edinbourgh (U.K., 1978), Katholieke Universiteit Leuven (Belgium, 1979), and Stanford University (California, 1980).

Mr. del Alamo is a member of the Electrochemical Society and the American Physical Society. In 1980, he received the First Prize of the 1980 IEEE Region 8 Undergraduate Student Paper Contest in Stuttgart (Germany). During the summer of 1983, he was a recipient of the Electrochemical Society Energy Research Summer Fellowship Award, given by the Electrochemical Society.

*

Richard M. Swanson (S'67-M'78) was born in Davenport, IA, on May 13, 1945. He received the B.S.E.E. and M.S.E.E. degrees from Ohio State University in 1969 and the Ph.D. degree from Stanford University in 1974. His dissertation research concerned the modeling and fabrication of complementary MOS integrated circuits for micropower applications and resulted in the theories and first experimental data on threshold adjustment by ion implantation and the operation of MOS transistors in the "weak inversion" regime. He was a National Science Foundation fellow while at Stanford.

While finishing his dissertation, he worked at Hewlet-Packard Laboratories, developing silicon-on-insulating-substrate technology. He received an IBM post-doctoral fellowship in 1974 at Stanford University to study techniques for solar-electric power generation. In 1976, he joined the faculty at Stanford as an Assistant Professor of Electrical Engineering and obtained funding from the Electric Power Research Institute to research thermophotovoltaic energy conversion for solar applications. Since then he has been actively involved in photovoltaics research. He is presently an Associate Professor of Electrical Engineering at Stanford University and heads a photovoltaics research team consisting of nine doctoral students, a research associate, an R&D engineer, and a processing technician. He has published over 50 technical papers.

Dr. Swanson is a member of the American Physical Society, the Electrochemical Society, the AAAS, the International Solar Energy Society, Sigma Chi, Tau Beta Pi, and Eta Kappa Nu.